

Tilted-Cone-induced easy-plane pseudo-spin ferromagnet and Kosterlitz-Thouless transition in massless Dirac fermions

Akito KOBAYASHI^{1,2}, Yoshikazu SUZUMURA², Hidetoshi FUKUYAMA³, and
Mark O. GOERBIG⁴

¹*Institute for Advanced Research, Nagoya University, Furo-cho, Chikusa-ku, Nagoya, 464-8602 Japan*

²*Department of Physics, Nagoya University, Furo-cho, Chikusa-ku, Nagoya, 464-8602 Japan*

³*Department of Applied Physics, Tokyo University of Science, 1-3, Kagurazaka, Shinjuku-ku, Tokyo
162-8601 Japan*

⁴*Laboratoire de Physique des Solides, CNRS UMR 8502, Universite Paris-Sud, F-91405 Orsay Cedex,
France*

The possible quantum Hall ferromagnet at a filling factor $\nu = 0$ is investigated for the zero-energy ($N = 0$) Landau level of the two dimensional massless Dirac fermions in α -(BEDT-TTF)₂I₃ under pressure with tilted cones and a twofold valley degeneracy resulting from time-reversal symmetry. In the case of the Dirac cones without tilting, the long-range Coulomb interaction in the $N = 0$ Landau level exhibits the $SU(2)$ valley-pseudo-spin symmetry even to the order $O(a/l_H)$, in contrast to $N \neq 0$ Landau levels, where a and l_H represent the lattice constant and the magnetic length, respectively. Such a characteristic comes from a fact that zero-energy states in a particular valley are restricted to only one of the spinor components, whereas the other spinor component is necessarily zero. In the case of the tilted Dirac cones as found in α -(BEDT-TTF)₂I₃, one obtains a non-zero value of the second component and then the backscattering processes between valleys becomes non-zero. It is shown that this fact can lead to easy-plane pseudospin ferromagnetism (XY-type). In this case, the phase fluctuations of the order parameters can be described by the XY model leading to Kosterlitz-Thouless transition at lower temperature. In view of these theoretical results, experimental findings in resistivity of α -(BEDT-TTF)₂I₃ are discussed.

KEYWORDS: massless Dirac fermion, Weyl equation, zero-gap state, α -(BEDT-TTF)₂I₃, graphene, magnetic field, Landau level, electron correlation, quantum Hall ferromagnet, Kosterlitz-Thouless transition

§1. Introduction

The massless Dirac fermions in the quasi-two-dimensional organic conductor α -(BEDT-TTF)₂I₃,¹⁾ which obey the tilted Weyl equation^{2,3)}, have attracted much interest because of the mysteries of the experimental findings such as the weak temperature (T) dependence of resistivity (close to h/e^2), the strong T -dependence of the Hall coefficient,⁴⁻⁷⁾ and the two-step increase of resistivity with decreasing T in the presence of the magnetic field.⁵⁾

In the absence of magnetic field and under pressure $P = 18\text{kbar}$, the in-plane resistivity decreases weakly with decreasing T from the room temperature and turns to increase below the onset temperature, 10K, and then it saturates in the limit of $T \rightarrow 0$.⁵⁾ The origin of such weak but obvious T -dependence has not been elucidated yet. In the presence of magnetic field, H , perpendicular to the conducting plane, the two-step increase of resistivity is observed.⁵⁾ For example at $H = 10\text{T}$, with decreasing T , the resistivity decreases weakly from room temperature and turns to increase below $T_0 \cong 20\text{K}$ with the plateau in the lower temperature region. Another relative sharp increase is observed around $T_l \cong 5\text{K}$ leading to apparent saturation as $T \rightarrow 0$. Both T_0 and T_l increase with increasing magnetic field.

In the absence of tilting it has been established that the energy spectrum of the massless Dirac fermions becomes discrete by the Landau quantization owing to the orbital motion in the magnetic field, $E_N = \text{sgn}(N)\sqrt{2\hbar v^2 eH|N|}/c$, where v is the velocity, and N is an integer. Each Landau level has large degeneracy proportional to H , and is split into two states with up and down spins by the Zeeman energy, as shown in Fig. 1. The effects of tilting have been investigated recently and it is found that the Landau-level structure is qualitatively the same and that the effects of tilting are incorporated as modifications of effective velocity. By use of values of relevant parameters appropriate for α -(BEDT-TTF)₂I₃,^{3,8)} $E_1 \cong 5\text{meV}$ and $2E_Z \equiv g\mu_B H \cong 1\text{meV}$ with the g-factor $g = 2$ for $H=10\text{T}$. Hence we see that the energy scale seen in resistivity measurement, T_0 ($\cong 2\text{meV}$) and T_l , are smaller than E_1 . Thus, the observed two-step increase of resistivity in α -(BEDT-TTF)₂I₃ may be attributed to the $N = 0$ Landau levels, whose causes will be studied theoretically in this paper.

The long range Coulomb interaction plays an important role for massless Dirac fermions. The effective Coulomb interaction under magnetic field, I , is estimated as $I \cong e^2/\epsilon l_H \cong 50\sqrt{H[\text{T}]/\epsilon} \text{meV}$, where l_H is the magnetic length, $l_H = \sqrt{\hbar c/eH}$. Although the polarizability ϵ of α -(BEDT-TTF)₂I₃ under high pressure has not been identified so far and then there is some ambiguity, it is demonstrated later that $N = 0$ Landau states have instability toward the pseudo-spin ferromagnetism since the effective Coulomb interaction I can exceed $2E_z$. In the presence of tilting, it is shown that the electron correlation can give rise to the quantum Hall ferromagnet of the pseudo-spin (the degree of freedom on the valleys) with the help of the large degeneracy of the Landau levels. The easy plane anisotropy of the pseudo-spin

ferromagnet results from the back scattering processes which is the inter-valley scattering terms exchanging large momentum. Moreover, it is shown that the effects of fluctuations of phase variables of the order parameters can be described by XY Heisenberg model leading to Kosterlitz-Thouless (KT) transition⁹⁾ at lower temperature.

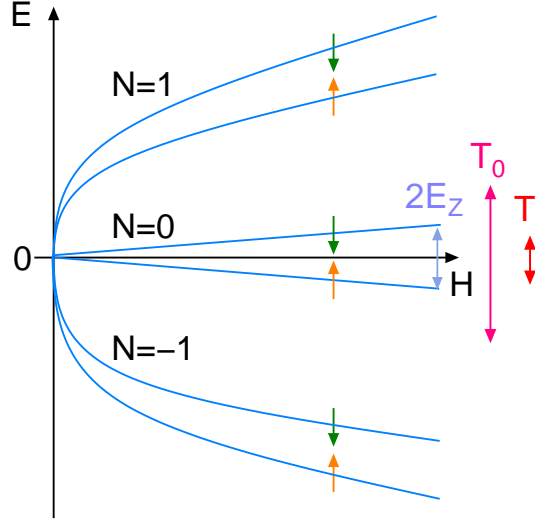


Fig. 1. Schematic figure of the Landau levels as a function of magnetic field. The energy scale of the onset temperature of the first increase of resistivity, T_0 , is located between the Zeeman gap $2E_Z$ and the $E_1 - E_0$ gap, where the Boltzmann factor k_B is taken as unit. The energy scale of the second increase of resistivity at low temperatures, T_l , is smaller than the Zeeman gap.

§2. Formulation

2.1 Hamiltonian for massless Dirac fermions with tilting

In the absence of magnetic field, the Hamiltonian of the massless Dirac fermions is given by,

$$\begin{aligned}
 \mathcal{H} &= \mathcal{H}_0 + \mathcal{H}', \\
 \mathcal{H}_0 &= \sum_{\mathbf{k}\gamma\gamma'\sigma\tau} [\mathcal{H}_0^{\sigma\tau}]_{\gamma\gamma'} c_{\mathbf{k}\gamma\sigma\tau}^\dagger c_{\mathbf{k}\gamma'\sigma\tau} \\
 \mathcal{H}' &= \frac{1}{2} \int \int d\mathbf{r} d\mathbf{r}' V_0(\mathbf{r} - \mathbf{r}') n(\mathbf{r}) n(\mathbf{r}')
 \end{aligned} \tag{1}$$

with the long-range Coulomb interaction $V_0(\mathbf{r}) = e^2/\epsilon r$ and the density operator $n(\mathbf{r})$. The degree of freedom on the spins are represented as $\sigma = \pm$ corresponding to \uparrow, \downarrow . The

degree of freedom of the pseudo-spins, $\tau = \pm$, corresponds to the valleys R, L . The valleys are located at the crossing points of the conduction and valence bands, $\pm \mathbf{k}_0$, where \mathbf{k}_0 is an incommensurate momentum in the first Brillouin zone.¹⁾ The creation and annihilation operators, $c_{\mathbf{k}\gamma\sigma\tau}^\dagger$ and $c_{\mathbf{k}\gamma\sigma\tau}$, respectively, are based on the Luttinger-Kohn representation¹⁰⁾ using the Bloch's functions at the crossing points as the basis of wave functions,²⁾ and then $\gamma = 1, 2$ denotes the basis of the Luttinger-Kohn representation. The relation between the Luttinger-Kohn representation and the site representation based on the molecular orbitals are described in Appendix. The low-energy properties around the two crossing points, labeled by $\tau = \pm$, are described in terms of the two tilted Weyl Hamiltonians^{2, 3)}

$$\begin{aligned} H_0^{\sigma, \tau=+} &= \hbar(v\mathbf{k} \cdot \boldsymbol{\sigma} + \mathbf{w}_0 \cdot \mathbf{k}\sigma_0) \\ H_0^{\sigma, \tau=-} &= -\hbar(v\mathbf{k} \cdot \boldsymbol{\sigma}^* + \mathbf{w}_0 \cdot \mathbf{k}\sigma_0) \end{aligned} \quad (2)$$

with respect to the time-reversal symmetry, where v represents the velocity of the cone and \mathbf{w}_0 represents the tilting velocity. Here, we have neglected the anisotropy of the velocity of the cone. In the case of the cone with anisotropic the velocity, one needs to replace $v\mathbf{k} \rightarrow (v_x k_x, v_y k_y)$.

Once a magnetic field perpendicular to the conducting plane is taken into account, the momentum \mathbf{k} is replaced by $\mathbf{k} + (e/c)\mathbf{A}$ with the vector potential in the Landau gauge $\mathbf{A} = (0, Hx, 0)$, and then we obtain

$$\begin{aligned} H_0^{\sigma, \tau=+} &= \begin{bmatrix} \hbar\{w_{0x}\frac{1}{i}\frac{\partial}{\partial x} + w_{0y}(\frac{1}{i}\frac{\partial}{\partial y} + \frac{eHx}{c})\} - \sigma E_Z & \hbar v\{\frac{1}{i}\frac{\partial}{\partial x} - i(\frac{1}{i}\frac{\partial}{\partial y} + \frac{eHx}{c})\} \\ \hbar v\{\frac{1}{i}\frac{\partial}{\partial x} + i(\frac{1}{i}\frac{\partial}{\partial y} + \frac{eHx}{c})\} & \hbar\{w_{0x}\frac{1}{i}\frac{\partial}{\partial x} + w_{0y}(\frac{1}{i}\frac{\partial}{\partial y} + \frac{eHx}{c})\} - \sigma E_Z \end{bmatrix} \\ H_0^{\sigma, \tau=-} &= \begin{bmatrix} \hbar\{w_{0x}\frac{1}{i}\frac{\partial}{\partial x} + w_{0y}(\frac{1}{i}\frac{\partial}{\partial y} + \frac{eHx}{c})\} - \sigma E_Z & \hbar v\{-\frac{1}{i}\frac{\partial}{\partial x} - i(\frac{1}{i}\frac{\partial}{\partial y} + \frac{eHx}{c})\} \\ \hbar v\{-\frac{1}{i}\frac{\partial}{\partial x} + i(\frac{1}{i}\frac{\partial}{\partial y} + \frac{eHx}{c})\} & \hbar\{w_{0x}\frac{1}{i}\frac{\partial}{\partial x} + w_{0y}(\frac{1}{i}\frac{\partial}{\partial y} + \frac{eHx}{c})\} - \sigma E_Z \end{bmatrix} \end{aligned} \quad (3)$$

in terms of the Zeeman energy E_Z .

2.2 Zero-energy Landau level for the case with tilting

The eigen equations for the zero-energy Landau level are given by

$$H_0^{\sigma, \tau} \phi_X^\tau(\mathbf{r}) = 0 \quad (4)$$

which gives the eigen functions of the tilted Weyl Hamiltonians in the presence of magnetic field. The wave functions are given by³⁾

$$\phi_X^\tau(\mathbf{r}) = \frac{1}{\sqrt{L}} e^{-iXy/l_H^2} \varphi^\tau(x - X) e^{-i\tau \mathbf{k}_0 \cdot \mathbf{r}} \quad (5)$$

with

$$\varphi^\tau(x) = \frac{1}{\sqrt{\sqrt{\pi/\gamma} l_H}} \chi_\tau e^{-\gamma x^2/2l_H^2}, \quad (6)$$

where X is the guiding-center coordinate and L is the length of the system. The spinor parts χ_τ are given by

$$\chi_{\tau=+} = \frac{1}{\sqrt{\tilde{w}_0^2 + (1 + \gamma)^2}} \begin{pmatrix} -\tilde{w}_0 e^{-i\varphi} \\ 1 + \gamma \end{pmatrix}, \quad (7)$$

$$\chi_{\tau=-} = \frac{1}{\sqrt{\tilde{w}_0^2 + (1 + \gamma)^2}} \begin{pmatrix} 1 + \gamma \\ -\tilde{w}_0 e^{+i\varphi} \end{pmatrix}. \quad (8)$$

Here, we have defined

$$\tilde{w}_0 e^{i\varphi} \equiv \frac{w_{0x} + iw_{0y}}{v}, \quad (9)$$

in terms of the effective tilting parameter

$$\tilde{w}_0 \equiv \sqrt{\left(\frac{w_{0x}}{v}\right)^2 + \left(\frac{w_{0y}}{v}\right)^2} \quad (10)$$

with $\mathbf{w}_0 = (w_{0x}, w_{0y})$, and $\gamma = \sqrt{1 - \tilde{w}_0^2}$. We note that one recovers the usual result for the $n = 0$ wave function in graphene when we use in the limit $\tilde{w}_0 \rightarrow 0$ ($\gamma \rightarrow 1$), i.e. in the case without tilting.

2.3 Effective Hamiltonian on fictitious magnetic lattice

We consider the present model by using the bases of the Wannier functions for the magnetic rectangular lattice which is introduced fictitiously. The wave functions in the Landau gauge are not localized in the y -direction, but in the x -direction around the position X . By applying the periodic boundary condition in the y -direction with the system length L , the X is discretized as $X = -2\pi l_H^2 j / L$ with an integer j . The Wannier functions, which satisfy orthonormality and are localized around $\mathbf{R} = (ma, nb)$ with integers m and n as shown in Fig. 2, are constructed by the linear combination of $\phi_X(\mathbf{r})$,¹¹⁾

$$\Phi_{\mathbf{R}}^\tau(\mathbf{r}) = \frac{\sqrt{L}}{a\sqrt{b}} \int_{-a/2}^{a/2} dX e^{iXnb/l_H^2} \phi_{X+ma}^\tau(\mathbf{r}), \quad (11)$$

where a is arbitrary but $a \gg 2\pi l_H^2 / L$ and $b = 2\pi l_H^2 / a$. We note that $|\Phi_{\mathbf{R}}^\tau(\mathbf{r})|$ exhibits an exponential-like decrease in the x -direction, but decreases algebraically as $|y|^{-1}$ in the y -direction.

In the basis of these Wannier functions, the effective interaction Hamiltonian is given by

$$\begin{aligned} \mathcal{H}'_{N=0} &= \frac{1}{2} \sum_{\mathbf{R}_{1,2,3,4}} \sum_{\sigma\sigma'\tau_{1,2,3,4}} \int \int d\mathbf{r} d\mathbf{r}' V_0(\mathbf{r} - \mathbf{r}') \\ &\times \left[\Phi_{\mathbf{R}_1}^{\tau_1}(\mathbf{r})^\dagger \cdot \Phi_{\mathbf{R}_2}^{\tau_2}(\mathbf{r}) \right] \left[\Phi_{\mathbf{R}_3}^{\tau_3}(\mathbf{r}')^\dagger \cdot \Phi_{\mathbf{R}_4}^{\tau_4}(\mathbf{r}') \right] \\ &\times c_{\mathbf{R}_1\sigma\tau_1}^\dagger c_{\mathbf{R}_2\sigma\tau_2} c_{\mathbf{R}_3\sigma'\tau_3}^\dagger c_{\mathbf{R}_4\sigma'\tau_4} \end{aligned} \quad (12)$$

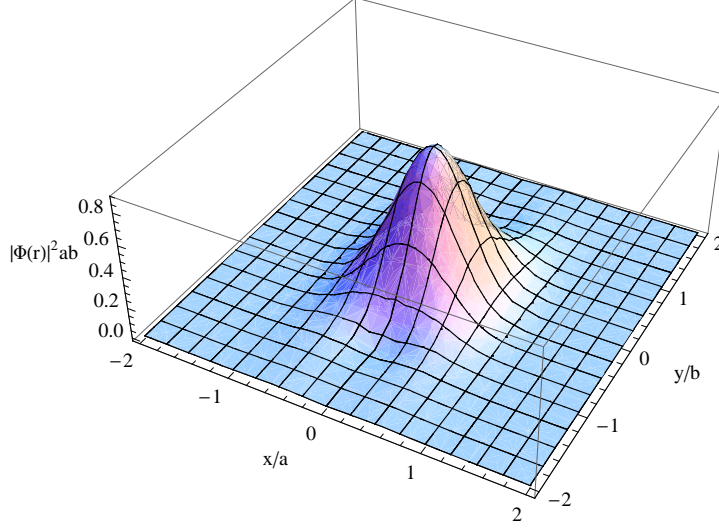


Fig. 2. The \mathbf{r} -dependence of $|\Phi_{\mathbf{R}}^{\tau}(\mathbf{r})|^2$ with $\mathbf{R} = \mathbf{0}$, where $\Phi_{\mathbf{R}}^{\tau}(\mathbf{r})$ is the Wannier functions for the magnetic rectangular lattice.

under the assumption that the density operator is effectively determined by the field operator for $N = 0$ Landau states and the contributions to the Hamiltonian from $N \neq 0$ states are negligible, *i. e.* we use the density operator

$$n(\mathbf{r}) = \sum_{\mathbf{R}\mathbf{R}'\sigma\tau\tau'} \left[\Phi_{\mathbf{R}}^{\tau}(\mathbf{r})^{\dagger} \cdot \Phi_{\mathbf{R}'}^{\tau'}(\mathbf{r}) \right] c_{\mathbf{R}\sigma\tau}^{\dagger} c_{\mathbf{R}'\sigma'\tau'}. \quad (13)$$

Thus the effective Hamiltonian for the $N = 0$ Landau states in the magnetic rectangular lattice is given by

$$\begin{aligned} \mathcal{H}_{\text{eff}} = & \sum_{i\sigma\tau} (-\sigma E_Z) c_{i\sigma\tau}^{\dagger} c_{i\sigma\tau} \\ & + \sum_{ijkl\sigma\sigma'\tau\tau'} V_{ijkl} c_{i\sigma\tau}^{\dagger} c_{j\sigma\tau} c_{k\sigma'\tau'}^{\dagger} c_{l\sigma'\tau'} \\ & + \sum_{ijkl\sigma\sigma'\tau} W_{ijkl} c_{i\sigma\tau}^{\dagger} c_{j\sigma\tau} c_{k\sigma'\tau}^{\dagger} c_{l\sigma'\bar{\tau}}, \end{aligned} \quad (14)$$

where i, j, k , and l denote the unit cells of the magnetic rectangular lattice at $\mathbf{R}_i, \mathbf{R}_j, \mathbf{R}_k$, and \mathbf{R}_l , respectively, and $\bar{\tau} = -\tau$.

The forward-scattering term, V_{ijkl} , is given by

$$V_{ijkl} = \frac{1}{2} \int \int d\mathbf{r} d\mathbf{r}' V_0(\mathbf{r} - \mathbf{r}') \left[\Phi_i^{\tau}(\mathbf{r})^{\dagger} \cdot \Phi_j^{\tau}(\mathbf{r}) \right] \left[\Phi_k^{\tau'}(\mathbf{r}')^{\dagger} \cdot \Phi_l^{\tau'}(\mathbf{r}') \right] \quad (15)$$

from the long wave length part of $\mathcal{H}'_{N=0}$. This term does not depend on the spin and pseudo-spin, and then it does not break the SU(4) symmetry, neither in the spin subspace nor in

that of the pseudo-spin. We find that the forward-scattering term is not affected by the tilting, because $(\chi_\tau^\dagger \cdot \chi_\tau)(\chi_{\tau'}^\dagger \cdot \chi_{\tau'}) = 1$.

On the other hand, the backscattering term, W_{ijkl} , which is the inter-valley scattering term exchanging large momentum $2k_0$ and breaks the SU(2) symmetry in the subspace of the pseudo-spin, is given by

$$W_{ijkl} = \frac{1}{2} \int \int d\mathbf{r} d\mathbf{r}' V_0(\mathbf{r} - \mathbf{r}') [\Phi_i^\dagger(\mathbf{r}) \cdot \Phi_j^\dagger(\mathbf{r})] [\Phi_k^\dagger(\mathbf{r}') \cdot \Phi_l^\dagger(\mathbf{r}')] \quad (16)$$

from the short wave length part of $\mathcal{H}'_{N=0}$. In the absence of tilting, as e.g. in graphene, the backscattering term vanishes because $(\chi_\tau^\dagger \cdot \chi_\tau) = 0$.¹²⁾ We find that the tilting is essential to have a non-zero backscattering term. The tilting dependence of the backscattering term is given by the spinor part,

$$(\chi_\tau^\dagger \cdot \chi_\tau)(\chi_\tau^\dagger \cdot \chi_{\bar{\tau}}) = \frac{4\tilde{w}_0^2(1+\gamma)^2}{[\tilde{w}_0^2 + (1+\gamma)^2]^2} \simeq 4\tilde{w}_0^2 + O(\tilde{w}_0^4), \quad (17)$$

where the last step has been obtained from the limit $\tilde{w}_0 \ll 1$. The ratio between the forward and the backscattering terms, W_{ijkl}/V_{ijkl} , is given by

$$W_{ijkl}/V_{ijkl} \simeq \frac{\tilde{w}_0^2 a_L}{l_H}, \quad (18)$$

where a_L is the lattice constant in the conducting plane. The backscattering term is proportional to a_L , since the large momentum $|2k_0| \cong \pi/a_L$ is exchanged.¹²⁾ We note that the lattice constant of α -(BEDT-TTF)₂I₃, $a_L \cong 10\text{\AA}$, is much larger than that of graphene. Thus it is expected that the backscattering term plays an important role for electron-correlation effects in α -(BEDT-TTF)₂I₃. The typical value of the ratio W_{ijkl}/V_{ijkl} is approximately 0.07 for α -(BEDT-TTF)₂I₃ at $H = 10\text{T}$ using the tilting parameter $\tilde{w}_0 \cong 0.8$. The Umklapp scattering term ($\tau\bar{\tau}\tau\bar{\tau}$ -term) can be neglected, because it is exponentially smaller than the other terms as a function of a_L/l_H , which is estimated as 0.1 at $H = 10\text{T}$ in α -(BEDT-TTF)₂I₃.

§3. Pseudo-spin ferromagnet and Kosterlitz-Thouless transition

Possible spin and pseudo-spin ferromagnetic states in the zero-energy Landau level in graphene have been extensively studied in recent years.¹²⁻¹⁹⁾ Generically, the ferromagnetic ordering may be understood within an interaction model with no explicit spin or pseudo-spin symmetry breaking; in order to minimize their exchange energy, the global N -particle wave function should be fully antisymmetric in its orbital part, the (pseudo-)spin part needs to be fully symmetric in order to fulfil fermionic statistics. Whereas in a normal metal this ordering is only partial, due to the increase in the kinetic energy, a single Landau level may be viewed as an infinitely flat energy band, and the ferromagnetic ordering may therefore be

complete. In the absence of an explicit symmetry breaking, such as the Zeeman effect that naturally tends to polarize the physical spin or the above-mentioned backscattering term that affects the pseudo-spin, no particular spin or pseudo-spin channel is selected, and one may even find an entangled spin-pseudo-spin ferromagnetic state.²⁰⁾ The symmetry-breaking terms may, thus, be viewed as ones that choose a particular channel (spin or pseudo-spin) and direction of a pre-existing ferromagnetic state by explicitly breaking the original SU(4) symmetry.

3.1 Mean-field solution

The mean-field Hamiltonian for the pseudo-spin ferromagnetic state is given by

$$\begin{aligned} \mathcal{H}_{\text{MF}} = & \sum_{j\sigma\tau} \left[-\sigma E_Z - 2 \sum_i (V_{ijji} n_{i\sigma\tau} + W_{ijji} n_{i\sigma\bar{\tau}}) \right] c_{j\sigma\tau}^\dagger c_{j\sigma\tau} \\ & - 2 \sum_{ij\sigma\tau} (V_{ijji} + W_{ijji}) (\langle c_{i\sigma\tau}^\dagger c_{i\sigma\bar{\tau}} \rangle c_{j\sigma\bar{\tau}}^\dagger c_{j\sigma\tau} + \text{h.c.}) \end{aligned} \quad (19)$$

and the order parameter of the pseudo-spin ferromagnetic state, Δ , which is independent of i and σ , is defined by

$$\Delta = 2I \langle c_{i\sigma-}^\dagger c_{i\sigma+} \rangle \quad (20)$$

with the effective interaction $I = \sum_i (V_{i00i} + W_{i00})$. Using the spin polarization, $m = \sum_{\sigma\tau} \sigma n_{i\sigma\tau}$, which is also independent of i , and the renormalized Zeeman energy, $\tilde{E}_Z = E_Z + mI$, the mean-field Hamiltonian is given by

$$\begin{aligned} \mathcal{H}_{\text{MF}} = & \sum_j \mathbf{c}_j^\dagger \hat{\mathcal{H}} \mathbf{c}_j \\ \hat{\mathcal{H}} = & \begin{bmatrix} -\tilde{E}_Z & -\Delta^* & 0 & 0 \\ -\Delta & -\tilde{E}_Z & 0 & 0 \\ 0 & 0 & \tilde{E}_Z & -\Delta^* \\ 0 & 0 & -\Delta & \tilde{E}_Z \end{bmatrix} \end{aligned}$$

with $\mathbf{c}_j = (c_{j\uparrow+}, c_{j\uparrow-}, c_{j\downarrow+}, c_{j\downarrow-})$. The mean-field solution is calculated from

$$|\Delta| = \frac{2I}{\pi} \int dx f(x) \text{Im} \frac{|\Delta|}{(x + i\delta - \sigma \tilde{E}_Z)^2 - |\Delta|^2} \quad (21)$$

and

$$m = \frac{1}{2} \sum_{\sigma\tau} \sigma f(-\sigma \tilde{E}_Z + \tau |\Delta|) \quad (22)$$

with the Fermi distribution function, $f(x)$.

The ground state in the case with $I < E_Z$ is a spin polarized state without pseudo-spin polarization ($m = 1$ and $\Delta = 0$ at $T = 0$), where electrons reside in the spin-up branches of the $N = 0$ Landau levels (see the left hand side of fig. 3(a)). The ground state in the case

with $I > E_Z$ is, on the other hand, a pseudo-spin ferromagnetic state ($m = 0$ and $|\Delta| = I$ at $T = 0$), where the easy-plane pseudo-spin polarization lifts the pseudo-spin degeneracy and then the spin polarization is suppressed (see the right hand side of fig. 3(a)).

The mean-field phase diagram in the I - T plane scaled by E_Z is shown in fig. 3(b). The transition temperature for the easy-plane pseudo-spin ferromagnetic state, T_c , is finite in the case with $I > E_Z$, and increases with increasing I . Below T_c , the spin polarization vanishes at $T \rightarrow 0$, although it is still finite at finite temperatures.

One notices that this competition between a spin polarized state and an easy-plane pseudo-spin ferromagnetism is original to the filling factor $\nu = 0$, where necessarily two (of four) subbranches of the zero-energy Landau levels are occupied. In contrast to this particular filling factor, this competition is absent at $\nu = \pm 1$, where only one subbranch is occupied and where, therefore, a spin polarization does not exclude a simultaneous pseudo-spin ordering in a coherent superposition of both pseudo-spin states.

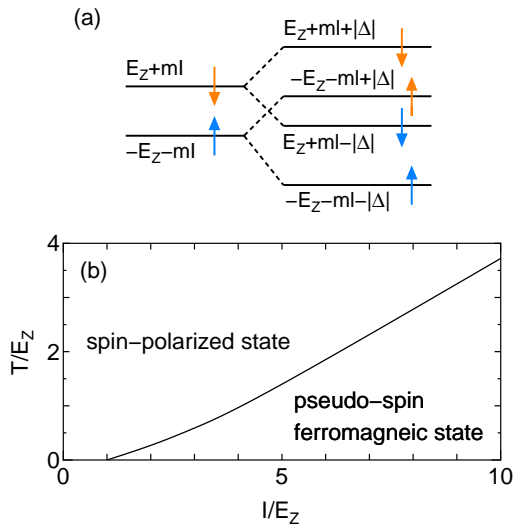


Fig. 3. (a) Schematic figure of the energy levels in the spin-polarized state (left hand side) and the pseudo-spin ferromagnetic state (right hand side). (b) Phase diagram in the plane of the interaction I and temperature T scaled by the Zeeman energy E_Z .

3.2 Phase fluctuations and Kosterlitz-Thouless transition

In the presence of an order parameter with a finite amplitude below T_c , phase fluctuation exists with the characteristic length of spatial variation much longer than the fictitious lattice

spacing. The effect of these phase fluctuation, which has so far been ignored in the mean-field approximation, is treated on the basis of the Wannier functions and the resulting model is similar to the XY model leading to the KT transition. Using the pseudo-spin operator, $\tilde{S}_{i-}^\sigma \equiv c_{i\sigma L}^\dagger c_{i\sigma R}$, and the real spin operator, $S_{jz} = \frac{1}{2} \sum_{\sigma\tau} \sigma c_{j\sigma\tau}^\dagger c_{j\sigma\tau}$, the mean-field Hamiltonian is given by

$$\begin{aligned} \mathcal{H}_{\text{MF}} = & -2(E_Z + mI) \sum_j S_{jz} \\ & - 2 \sum_{ij\sigma} I_{ij} \left(\langle \tilde{S}_{i-}^\sigma \rangle \tilde{S}_{j+}^\sigma + \langle \tilde{S}_{i+}^\sigma \rangle \tilde{S}_{j-}^\sigma \right). \end{aligned} \quad (23)$$

The real spin polarization, m , remains finite at finite temperatures, although it vanishes at $T \rightarrow 0$ in the pseudo-spin ferromagnetic state. However, it can be shown that the spin polarization is independent of i , since the pseudo-spin can fluctuate only in the easy plane and then the occupation numbers of electrons are independent of i . The interactions between the pseudo-spins on the magnetic rectangular lattice, $I_{ij} \equiv V_{ijji} + W_{iijj}$. The interaction I_{ij} rapidly decreases with increasing $|\mathbf{R}_j - \mathbf{R}_i|$. It is numerically found as seen in Fig. 4 that the nearest-neighbor I_{ij} is approximately isotropic and the ratio $I_{i,i+1}/I_{i,i} = 0.10$ with the arbitrary choice of $b = \sqrt{2}a$ (but leading to the almost isotropic localization of the Wannier function on the fictitious lattice), where

$$\frac{I_{i,j}}{I_{i,i}} = \frac{V_{ijji} + W_{iijj}}{V_{iiii} + W_{iiii}} \cong \frac{V_{ijji}}{V_{iiii}} \quad (24)$$

The phase of the order parameter corresponds to the angles of the pseudo-spin. The x - and y -components of the pseudo-spins are given by $\langle \tilde{S}_{ix}^\sigma \rangle = \text{Re}\langle \tilde{S}_{i-}^\sigma \rangle$ and $\langle \tilde{S}_{iy}^\sigma \rangle = -\text{Im}\langle \tilde{S}_{i-}^\sigma \rangle$, respectively, with $\langle \tilde{S}_{i+}^\sigma \rangle = \langle \tilde{S}_{i-}^\sigma \rangle^*$. Thus $\langle \tilde{S}_{i-}^\sigma \rangle$ can be represented using the angle of the pseudo-spin from the x -direction in the x - y plane, ϕ_i^σ , as $\langle \tilde{S}_{i-}^\sigma \rangle = |\langle \tilde{S}_{i-}^\sigma \rangle| \exp(-i\phi_i^\sigma)$. When the characteristic length of spatial variation of the phases is much longer than the lattice spacing, we can expand the free energy by the fluctuations of the phases $f_{ij}^\sigma = 1 - \cos(\phi_j^\sigma - \phi_i^\sigma) \ll 1$ under the assumption that the amplitude, $|\langle \tilde{S}_{i-}^\sigma \rangle|$, does not change within the characteristic length of the phase fluctuation, and then we obtain

$$\begin{aligned} F_f - F_n & \cong (F_f - F_n)|_{f_{ij}^\sigma=0} + \sum_{\langle i \neq j \rangle \sigma} \frac{\partial (F_f - F_n)}{\partial f_{ij}^\sigma} f_{ij}^\sigma \\ & = F_0 - \sum_{\langle i \neq j \rangle \sigma} J_{ij}^\sigma \cos(\phi_j^\sigma - \phi_i^\sigma) \end{aligned} \quad (25)$$

with $J_{ij}^\sigma = 4|\langle \tilde{S}_{i-}^\sigma \rangle|^2 I_{ij}$, where F_f and F_n denote the free energies of the pseudo-spin ferromagnetic and normal states, respectively, and F_0 is independent of the phases. The effects of the phase fluctuations in J_{ij}^σ are neglected since those effects are the higher-order terms, and $J_{ij}^\sigma \rightarrow I_{ij}$ at temperatures much lower than T_c . Then the physics of the phase fluctuation is

equivalent to that of the two-dimensional XY Heisenberg model with the nearest-neighbor exchange interaction, $J \cong I_{i,i+1} \cong 0.087I$. In the two-dimensional XY model, the KT transition occurs due to the onset of bound pairs of the vortices.⁹⁾ It is known that $T_{\text{KT}} \cong 1.54J$ by the renormalization group analysis.²¹⁾ Here the effects of spin polarization are negligible, because J is much larger than the Zeeman energy and the phase fluctuation on each electron with up or down spin is described by the same interaction, J .

Lastly we discuss the role of the long-range part of I_{ij} farther than the nearest neighbor one. Figure 4 shows the distance dependences of $I_{0,j}/I_{0,0}$ with $\mathbf{R}_j = (na, 0)$ (the closed circles) and $\mathbf{R}_i = (0, nb)$ (the open circles) defined on an integer n , where we take $b = \sqrt{2}a$. The interaction I_{0j} decays very rapidly along the x -axis but slowly along y -axis. Then the role of the long range part of I_{ij} along y -axis should be considered for improving the effective Hamiltonian. The KT transition temperature T_{KT} , however, is determined by the competition between the excitation energy of a vortex and the entropy effect coming from the degree of freedom for the position of the vortex core. Since the length scale of the vortex is much longer than a and the interaction is ferromagnetic, the long-range part of I_{ij} does not disturb the KT transition essentially.

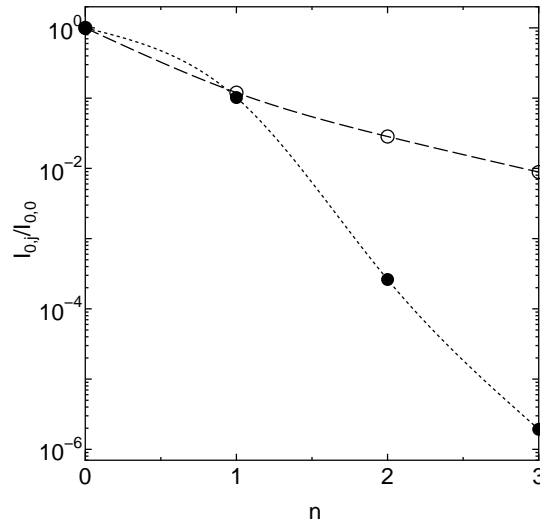


Fig. 4. The n -dependences of $I_{0,j}/I_{0,0}$ with $\mathbf{R}_j = (na, 0)$ (the closed circles) and $\mathbf{R}_i = (0, nb)$ (the open circles), where we take $b = \sqrt{2}a$. The dashed and dotted lines are a guide to the eye.

§4. Relation between Experimental Findings and Theoretical Results

In the presence of magnetic field perpendicular to the conducting plane, the two-step increase of resistivity, for example at $T_0 \cong 20\text{K}$ and $T_l \cong 5\text{K}$ at $H = 10\text{T}$, is observed in $\alpha\text{-(BEDT-TTF)}_2\text{I}_3$, where both T_0 and T_l increase with increasing magnetic field.⁵⁾ We may be able to associate two stepwise changes of resistivity as due to the easy-plane pseudo-spin ferromagnetic transition at T_c and the KT transition at T_{KT} , since our estimate indicates that $T_c \cong 4T_{\text{KT}}$, where $T_c \cong 0.5I$ as seen in Fig. 3(b) in the region of $I/E_Z \gg 1$ of interest and $T_{\text{KT}} \cong 1.54J \cong 0.13I$. We emphasize that the tilting of the Dirac cone is essential to the appearance of the easy-plane pseudo-spin ferromagnet, and thus, to the appearance of the KT transition, due to the long range Coulomb interaction.

§5. Conclusion and Discussion

In the present paper, motivated by the experimental observation of the particular temperature dependences of resistivity in $\alpha\text{-(BEDT-TTF)}_2\text{I}_3$ under magnetic field, the possibility of the pseudo-spin quantum Hall ferromagnet at $\nu = 0$ has been investigated in the massless Dirac fermion system. The pseudo-spin ferromagnetic transition occurs when the electron correlation exceeds the Zeeman energy. The tilting of the Dirac cone induces the backscattering terms resulting in the easy-plane pseudo-spin ferromagnet. There will be intrinsic fluctuations and T_c should be considered only as a crossover temperature for the growing amplitude of order parameters with remaining large phase fluctuations in the two-dimensional system. To treat such phase fluctuations, a spatially localized basis set similar to “Wannier function” are introduced, which indicates that the model is similar to the XY model which is known to lead to the KT transition at lower temperature, T_{KT} . In comparison with experiments, the two-step increase of resistivity with decreasing temperature are observed at around 20K and 5K at $H = 10\text{T}$. Present theory has revealed $T_{\text{KT}} \cong 5\text{K}$ on the choice of the parameters giving $T_c \cong 20\text{K}$, and then there are reasonable correspondences to identify two stepwise changes of resistivity as due to the amplitude growing and the phase coherence of the order parameters.

Obviously there are remaining problems to be clarified. The experimental data indicates the saturation of resistivity in the low temperature. The saturation indicates the existence of dilute carriers which may originate from weak three-dimensionality or disorder.

In graphene,²²⁾ the the quantum Hall ferromagnet at $\nu = 0$ has been investigated,^{12, 14, 13, 16, 19)} and very recently it is suggested that the electron-phonon interaction breaking the pseudo-spin SU(2) symmetry, which may be characteristic of graphene, induces the easy-plane pseudo-spin ferromagnet resulting in the KT transition²³⁾ in order to explain the possible KT transition observed in graphene.²⁴⁾ We emphasize that the backscattering term,

which is the key factor for the easy-plane pseudo-spin ferromagnet in our paper, is characteristic of α -(BEDT-TTF)₂I₃, but can be realized in graphene by distorting the honeycomb lattice. In addition, we note that a lattice model describing the fluctuations of the pseudo-spins should be based on Wannier functions which satisfy orthonormality under magnetic field, since the bases on the original crystal lattice are no longer the eigenstates of the $N = 0$ Landau levels.

The effects of the short range parts of the Coulomb interaction in graphene also have been investigated. If once the pseudo-spin ferromagnetism occurs, the Hubbard- U -type on-site interaction favors the easy-plane ferromagnetism (uniform charge density), while the nearest-neighbor interaction V favors the easy-axis ferromagnetism (the sublattice CDW), in the case of graphene.¹⁴⁾ In α -(BEDT-TTF)₂I₃, however, the easy-axis ferromagnetism does not correspond to CDW directly, because the bases of the Weyl Hamiltonian is not the sublattice but the Bloch states at $\mathbf{k} = \pm\mathbf{k}_0$. The Bloch states at $\mathbf{k} = \pm\mathbf{k}_0$ consist of the linear combination of the contributions from four BEDT-TTF molecules. Thus, although the easy-axis ferromagnetism may modify the intrinsic charge disproportionation in α -(BEDT-TTF)₂I₃, the effect of V on such state may be weaker than that of graphene. It is an interesting difference between graphene and α -(BEDT-TTF)₂I₃, and it will be investigated intensively in future.

Lastly, we discuss the renormalization of fluctuation in the pseudo-spin ferromagnet, which are very complicated and not captured on the mean-field level. In the absence of the Zeeman effect, the ferromagnetic moment may fluctuate in the SU(4) space at temperatures between T_c and a symmetry breaking temperature, T_{sb} , which is essentially given by the symmetry-breaking interaction energy, W_{ijkl} . The ferromagnetic moment may be forced in the easy-plane below T_{sb} . In the presence of the Zeeman effect, the situation is more complicated owing to the competition between W_{ijkl} and the Zeeman energy, E_Z . The results in the present paper, thus, identify a new research target, *i. e.* a two-dimensional SU(4) model with the symmetry-breaking terms.

Acknowledgments

The authors are thankful to N. Tajima for fruitful discussions. This work has been financially supported by Grant-in-Aid for Special Coordination Funds for Promoting Science and Technology (SCF), Scientific Research on Innovative Areas 20110002, and Scientific Research 19740205 from the Ministry of Education, Culture, Sports, Science and Technology in Japan.

1) S. Katayama, A. Kobayashi and Y. Suzumura, J. Phys. Soc. Jpn. **75** (2006) 054705.

2) A. Kobayashi, S. Katayama, Y. Suzumura and H. Fukuyama, J. Phys. Soc. Jpn. **76** (2007) 034711.

- 3) M. O. Goerbig, J. -N. Fuchs, G. Montambaux, and F. Piechon, Phys. Rev. B **78** (2008) 045415.
- 4) K. Kajita, T. Ojiro, H. Fujii, Y. Nishio, H. Kobayashi, A. Kobayashi and R. Kato, J. Phys. Soc. Jpn. **61** (1992) 23.
- 5) N. Tajima, S. Sugawara, M. Tamura, Y. Nishio and K. Kajita, J. Phys. Soc. Jpn. **75** (2006) 051010.
- 6) N. Tajima, S. Sugawara, R. Kato, Y. Nishio, and K. Kajita, Phys. Rev. Lett. **102** (2009) 176403.
- 7) A. Kobayashi, Y. Suzumura, and H. Fukuyama, J. Phys. Soc. Jpn. **77** (2008) 064718.
- 8) T. Morinari, T. Himura, and T. Tohyama, J. Phys. Soc. Jpn. **78** (2009) 023704.
- 9) J. M. Kosterlitz and D. J. Thouless, J. Phys. **C5** (1972) 124; *ibid.* **6** (1973) 1181.
- 10) J. M. Luttinger and W. Kohn, Phys. Rev. **97** (1955) 869.
- 11) H. Fukuyama, unpublished (1977) [Kotai-Butsuri, Vol. 12 (1977) p. 727, in Japanese].
- 12) M. O. Goerbig, R. Moessner, and B. Douçot, Phys. Rev. B **74** (2006) 161407.
- 13) K. Nomura and A. H. MacDonald, Phys. Rev. Lett. **96** (2006) 256602.
- 14) J. Alicea and M. P. A. Fisher, Phys. Rev. B **74** (2006) 075422.
- 15) K. Yang, S. Das Sarma, and A. H. MacDonald, Phys. Rev. B **74** (2006) 075423.
- 16) V. P. Gusynin, V. A. Miransky, S. G. Sharapov, and I. A. Shovkovy, Phys. Rev. B **74** (2006) 195429.
- 17) I. Herbut, Phys. Rev. B **75** (2007) 165411; Phys. Rev. B **76** (2007) 085432.
- 18) R. L. Doretto and C. Morais Smith, Phys. Rev. B **76** (2007) 195431.
- 19) M. Ezawa, J. Phys. Soc. Jpn. **76** (2007) 094701.
- 20) B. Douçot, M. O. Goerbig, P. Lederer, and R. Moessner, Phys. Rev. B **78** (2008) 195327.
- 21) J. M. Kosterlitz, J. Phys. **C7** (1974) 1046.
- 22) K. S. Novoselov, A. K. Geim, S. V. Morozov, D. Jiang, M. I. Katsnelson, I. V. Grigorieva, S. V. Dubonos, and A. A. Firsov, Nature **438** (2005) 197.
- 23) K. Nomura, S. Ryu, and D-H Lee, cond-mat/0906.0159
- 24) J. G. Checkelsky, L. Li, and N. P. Ong, Phys. Rev. Lett. **100** (2008) 206801, Phys. Rev. B **79** (2009) 115434.
- 25) T. Mori, A. Kobayashi, Y. Sasaki, H. Kobayashi, G. Saito and H. Inokuchi, Chem. Letters (1984) 957.
- 26) H. Seo, C. Hotta and H. Fukuyama, Chem. Rev. **104** (2004) 5005.
- 27) A. Kobayashi, S. Katayama, K. Noguchi and Y. Suzumura, J. Phys. Soc. Jpn. **73** (2004) 3135.
- 28) A. Kobayashi, S. Katayama, and Y. Suzumura, accepted to Science and Technology of Advanced Materials (STAM) Special Issue: Organic Conductors.

Appendix: Relation between Luttinger-Kohn Representation and Site Representation

A basic model describing the two-dimensional electronic system in α -(BEDT-TTF)₂I₃ is given by²⁵⁻²⁷⁾

$$\mathcal{H}_{\text{site}} = \sum_{(i\alpha:j\beta),\sigma} (t_{i\alpha;j\beta} a_{i\alpha\sigma}^\dagger a_{j\beta\sigma} + \text{h.c.}), \quad (\text{A}\cdot 1)$$

where i and j denote the unit cells, α, β ($=A, A', B$ and C) denote the molecular orbital sites in a unit cell, $a_{i\alpha\sigma}^\dagger$ denote the creation operators on the site representation, and $t_{i\alpha;j\beta}$ is the transfer energy between (i, α) site and (j, β) site. Using the Fourier transformation, we obtain

$$\begin{aligned}\mathcal{H}_{\text{site}} &= \sum_{\mathbf{k}\alpha\beta\sigma} \epsilon_{\alpha\beta\sigma}(\mathbf{k}) a_{\mathbf{k}\alpha\sigma}^\dagger a_{\mathbf{k}\beta\sigma} \\ \epsilon_{\alpha\beta}(\mathbf{k}) &= \sum_{\delta} t_{\alpha\beta} e^{i\mathbf{k}\cdot\delta},\end{aligned}\tag{A.2}$$

where δ denotes the vector representing the nearest neighbor of the unit cell. Such Hamiltonian (here we call it the site Hamiltonian) is diagonalized by the eigenvalue equation

$$\sum_{\beta=1}^4 \epsilon_{\alpha\beta\sigma}(\mathbf{k}) d_{\beta\gamma\sigma}(\mathbf{k}) = \xi_{\gamma\sigma}(\mathbf{k}) d_{\alpha\gamma\sigma}(\mathbf{k}),\tag{A.3}$$

where $\xi_{\gamma\sigma}$ are the eigenvalue with the descending order, $\xi_{1\sigma}(\mathbf{k}) > \xi_{2\sigma}(\mathbf{k}) > \xi_{3\sigma}(\mathbf{k}) > \xi_{4\sigma}(\mathbf{k})$, and $d_{\alpha\gamma\sigma}(\mathbf{k})$ ($\gamma = 1, 2, 3, 4$) are the corresponding eigenvectors. Here $\xi_{1\sigma}(\mathbf{k})$ and $\xi_{2\sigma}(\mathbf{k})$ are the conduction and valence bands, respectively, because there are six electrons in the four molecules, i.e., the 3/4-filled electronic system.

Expanding the site Hamiltonian in the linear order of momenta from $\pm\mathbf{k}'_0$ and using the Luttinger-Kohn representation based on the Bloch's functions at $\pm\mathbf{k}'_0$ (corresponding to $\tau = \pm$), we obtain the tilted Weyl Hamiltonians, where $\pm\mathbf{k}'_0$ are infinitesimally close to the crossing points $\pm\mathbf{k}_0$, respectively.^{2, 28)} Then the creation operators on the Luttinger-Kohn representation $c_{\mathbf{k}\gamma\sigma\tau}^\dagger$ are given by

$$c_{\mathbf{k}\gamma\sigma\tau}^\dagger = \sum_{\alpha} d_{\alpha\gamma\sigma}^*(\tau\mathbf{k}'_0) a_{\mathbf{k}\alpha\sigma}^\dagger.\tag{A.4}$$